A New Approach to the Photochemically Controlled Crown Ethers: (Tetramethylcyclobutadiene)cobalt Complexes with Benzo-15-Crown-5 and Dibenzo-18-Crown-6[†]

Dmitry S. Perekalin,[‡] Maria V. Babak,[‡] Valentin V. Novikov,[‡] Pavel V. Petrovskii,[‡] Konstantin A. Lyssenko,[‡] Maddalena Corsini,[§] Piero Zanello,[§] and Alexander R. Kudinov*,[‡]

A. N. Nesmeyanov Institute of Organoelement Compounds, Russian Academy of Sciences, 119991, Moscow, Russian Federation, and Dipartimento di Chimica, Università di Siena, 53100, Siena, Italy

The photochemical substitution of benzene in $[Cb^*Co(C_6H_6)]^+$ ($Cb^* = C_4Me_4$) with benzo-15-crown-5 (**1**) gives the corresponding π-complex $[Cb^*Co(\eta^6\text{-}C_6H_4(OCH_2CH_2OCH_2CH_2)_2O)]^+$ (**2**). A similar reaction with dibenzo-18-crown-6 (**3**) produces cation $[Cb^*Co(\eta^6\text{-}C_6H_4(OCH_2CH_2OCH_2CH_2O)_2C_6H_4)]^+$ (**4**). Arene exchange is reversible, and both **1** and **3** can be regenerated by irradiation of **2** and **4** with excess benzene. The reaction of $[Cb^*Co(C_6H_6)]^+$ with 0.5 equiv of **3** gives dinuclear complex $[trans\text{-}Cb^*Co(\mu\text{-}\eta^6,\eta^6\text{-}C_6H_4(OCH_2CH_2OCH_2CH_2O)_2C_6H_4)CoCb^*]^{2+}$ (**5**). The structures of cations **4** and **5** were confirmed by X-ray diffraction. The electrochemical behavior of complexes prepared was studied. The sodium-binding ability of cobalt complexes **2**, **4**, and **5** (determined by NMR titration; $K_a = 2500$, 800, and 50, respectively) was found to be much smaller than that of the free crown ethers **1** and **3** ($K_a = 200\,000$ and $5\,000\,000$). DFT calculations suggest that this decrease is mainly due to electrostatic repulsion of Co^+ and Na^+ centers.

Introduction

The design of photochemically controlled receptors for anions and cations is an intensively studied area of tremendous potential significance.[2] Particularly, much attention is paid to the photochemically active crown ethers, which are the most simple and important receptors.[3] The common approach in this area is the organic functionalization of the classic crown ethers with chromophoric substituents (e.g., anthracene,[3a,c] azobenzene,[3b] stilbene,[3f] or trityl[3g]). In contrast, to the best of our knowledge, organometallic modification was not previously used for this purpose.[4] Herein we describe a novel approach for the photo-

chemical control of benzocrown ethers based on the reversible π-complexation of benzene rings with cationic $[(ring)M]^+$ fragments.

Results and Discussion

Synthesis and X-ray Structures. We have recently developed convenient methods for the preparation of sandwich,[1,5] half-sandwich,[6] and carborane[7] derivatives of the $[Cb^*Co]^+$ fragment.[8] One of them is the arene exchange in cationic

* To whom correspondence should be addressed. E-mail: arkudinov@ineos.ac.ru.

(1) Loginov, D. A.; Pronin, A. A.; Shulpina, L. S.; Mutseneck, E. V.; Starikova, Z. A.; Petrovskii, P. V.; Kudinov, A. R. *Izv. Akad. Nauk, Ser. Khim.* **2008**, 535.

(2) de Silva, A. P.; Gunaratne, H. Q. N.; Gunnlaugsson, T.; Huxley, A. J. M.; McCoy, C. P.; Rademacher, J. T.; Rice, T. E. *Chem. Rev.* **1997**, 97, 1515.
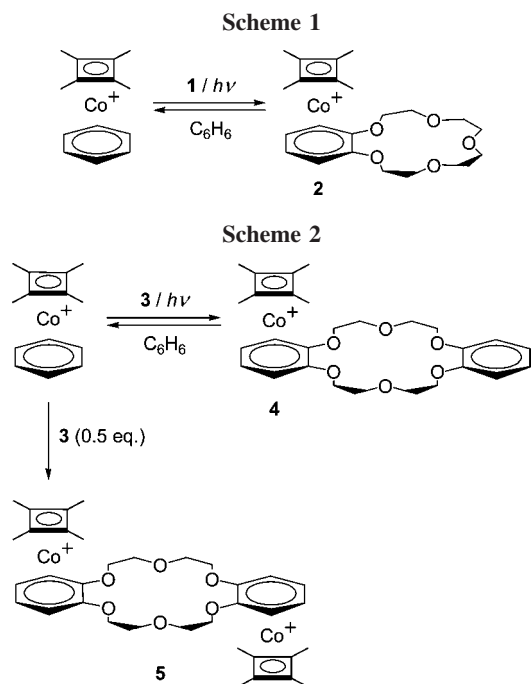
(3) For example see: (a) Desvergne, J.-P.; Bouas-Laurent, H. *J. Chem. Soc., Chem. Commun.* **1978**, 403. (b) Shinkai, S.; Minami, T.; Kusano, Y.; Manabe, O. *J. Am. Chem. Soc.* **1983**, 105, 1851. (c) Tucker, J. H. R.; Bouas-Laurent, H.; Marsau, P.; Rileya, S. W.; Desvergne, J.-P. *Chem. Commun.* **1997**, 1165. (d) Stauffer, M. T.; Knowles, D. B.; Brennan, C.; Funderburk, L; Lin, F-T.; Weber, S. G. *Chem. Commun.* **1997**, 287. (e) Kimura, K.; Mizutani, R.; Yokoyama, M.; Arakawa, R.; Matsubayashi, G.; Okamoto, M.; Doe, H. *J. Am. Chem. Soc.* **1997**, 119, 2062. (f) Alfimov, M. V.; Gromov, S. P.; Fedorov, Y. V.; Fedorova, O. A.; Vedernikov, A. I.; Churakov, A. V.; Kuz'mina, L. G.; Howard, J. A. K.; Bossmann, S.; Braun, A.; Woerner, M.; Sears, D. F., Jr.; Saltiel, J. *J. Am. Chem. Soc.* **1999**, 121, 4992. (g) Kimura, K.; Mizutani, R.; Yokoyama, M.; Arakawa, R.; Sakurai, Y. *J. Am. Chem. Soc.* **2000**, 122, 5448. (h) Malval, J.-P.; Gosse, I.; Morand, J.-P.; Lapouyade, R. *J. Am. Chem. Soc.* **2002**, 124, 904. (i) Fedorova, O. A.; Fedorov, Y. V.; Andrjukhina, E. N.; Gromov, S. P.; Alfimov, M. V. *Pure Appl. Chem.* **2003**, 75, 1077.

(4) The organometallic crown ethers were used as electrochemically active receptors and for other purposes. For example see: (a) Odell, K. J.; Hyde, E. M.; Shaw, B. L.; Shepherd, I. *J. Organomet. Chem.* **1979**, 168, 103. (b) Anson, C. E.; Creaser, C. S.; Stephenson, G. R. *J. Chem. Soc., Chem. Commun.* **1994**, 2175. (c) Plenio, H.; Burth, D. *Organometallics* **1996**, 15, 1151. (d) Beer, P. D. *Acc. Chem. Res.* **1998**, 31, 71. (e) Ballardini, R.; Balzani, V.; Clemente-Leon, M.; Credi, A.; Gandolfi, M. T.; Ishow, E.; Perkins, J.; Stoddart, F. J.; Tseng, H.-R.; Wenger, S. *J. Am. Chem. Soc.* **2002**, 124, 12786. (f) Amor, A. B. H.; Top, S.; Meganem, F.; Jaouen, G. *J. Organomet. Chem.* **2005**, 690, 847, and references therein. (g) Geldbach, T. J.; Brown, M. R. H.; Scopelliti, R.; Dyson, P. J. *J. Organomet. Chem.* **2005**, 690, 5055, and references therein.

(5) (a) Mutseneck, E. V.; Loginov, D. A.; Perekalin, D. S.; Starikova, Z. A.; Golovanov, D. G.; Petrovskii, P. V.; Zanello, P.; Corsini, M.; Laschi, F.; Kudinov, A. R. *Organometallics* **2004**, 23, 5944. (b) Mutseneck, E. V.; Petrovskii, P. V.; Kudinov, A. R. *Izv. Akad. Nauk, Ser. Khim.* **2004**, 2003; *Russ. Chem. Bull.* **2004**, 53, 2090 (Engl. Transl.). (c) Mutseneck, E. V.; Starikova, Z. A.; Lyssenko, K. A.; Petrovskii, P. V.; Zanello, P.; Corsini, M.; Kudinov, A. R. *Eur. J. Inorg. Chem.* **2006**, 4519.

(6) Butovskii, M. V.; Englert, U.; Fil'chikov, A. A.; Herberich, G. E.; Koelle, U.; Kudinov, A. R. *Eur. J. Inorg. Chem.* **2002**, 2656.

(7) (a) Kudinov, A. R.; Meshcheryakov, V. I.; Petrovskii, P. V.; Rybinskaya, M. I. *Iz V. Akad. Nauk, Ser. Khim.* **1999**, 177; *Russ. Chem. Bull.* **1999**, 48, 176 (Engl. Transl.). (b) Meshcheryakov, V. I.; Kitaev, P. S.; Lyssenko, K. A.; Starikova, Z. A.; Petrovskii, P. V.; Janouěk, Z.; Corsini, M.; Laschi, F.; Zanello, P.; Kudinov, A. R. *J. Organomet. Chem.* **2005**, 690, 4745. (c) Mutseneck, E. V.; Perekalin, D. S.; Holub, J.; Lyssenko, K. A.; Petrovskii, P. V.; Štíbr, B.; Kudinov, A. R. *Eur. J. Inorg. Chem.* **2006**, 1737. (d) Mutseneck, E. V.; Perekalin, D. S.; Holub, J.; Starikova, Z. A.; Petrovskii, P. V.; Zanello, P.; Corsini, M.; Štíbr, B.; Kudinov, A. R. *Organometallics* **2006**, 25, 2419.
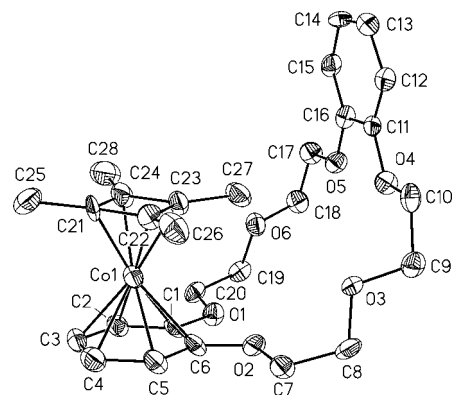
Scheme 1

Scheme 2

Figure 1. Molecular structure of cation **4** with 50% thermal ellipsoids. The hydrogen atoms are omitted for clarity. Selected interatomic distances (Å): Co1−C1 2.133(6), Co1−C2 2.142(5), Co1−C3 2.112(5), Co1−C4 2.120(5), Co1−C5 2.122(6), Co1−C6 2.140(6), Co1−C21 1.959(6), Co1−C22 1.977(6), Co1−C23 1.994(5), Co1−C24 1.982(6), Co1···C$_4$ 1.688, Co1···C$_6$ 1.599.
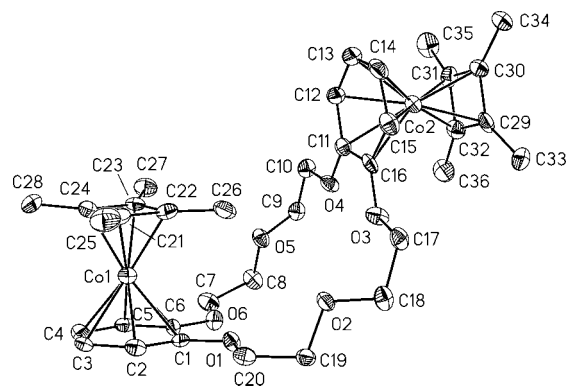
Figure 2. Molecular structure of dication **5** with 50% thermal ellipsoids. The hydrogen atoms and solvate acetone molecule are omitted for clarity. Selected interatomic distances (Å): Co1−C1 2.158(4), Co1−C2 2.108(4), Co1−C3 2.093(4), Co1−C4 2.094(4), Co1−C5 2.114(4), Co1−C6 2.131(4), Co1−C21 1.988(4), Co1−C22 1.985(4), Co1−C23 2.001(4), Co1−C24 1.988(4), Co2−C11 2.158(4), Co2−C12 2.086(4), Co2−C13 2.081(4), Co2−C14 2.084(4), Co2−C15 2.109(4), Co2−C16 2.166(4), Co2−C29 1.978(4), Co2−C30 1.977(4), Co2−C31 1.979(4), Co2−C32 1.982(4), Co1···C$_4$ 1.705, Co1···C$_6$ 1.577, Co2···C$_4$ 1.698, Co2···C$_6$ 1.574.

complexes [Cb*Co(arene)]$^+$ under visible light irradiation. Employing this method, the reaction of the benzene complex [Cb*Co(C$_6$H$_6$)]$^+$ with a 4-fold excess of benzo-15-crown-5 (**1**) gives the air- and moisture-stable complex [Cb*Co(η^6-C$_6$H$_4$(OCH$_2$CH$_2$OCH$_2$CH$_2$)$_2$O)]$^+$ (**2**) in 51% yield (Scheme 1).[9]

The analogous reaction of [Cb*Co(C$_6$H$_6$)]$^+$ with an excess of dibenzo-18-crown-6 (**3**) gives the mononuclear complex [Cb*Co(η^6-C$_6$H$_4$(OCH$_2$CH$_2$OCH$_2$CH$_2$O)$_2$C$_6$H$_4$)]$^+$ (**4**) in 71% yield (Scheme 2). Interestingly, the same reaction with an excess of the benzene complex results mainly in the dinuclear derivative [*trans*-Cb*Co(μ-η^6,η^6-C$_6$H$_4$(OCH$_2$CH$_2$OCH$_2$CH$_2$O)$_2$C$_6$H$_4$)Co-Cb*]$^{2+}$ (**5**) isolated in 55% yield. An admixture (<10%) of the *cis*-isomer is easily removed by fractional crystallization.

Importantly, photochemical arene exchange is reversible and can be easily controlled by concentration of the incoming arene (C$_6$H$_6$ or benzocrown ether). Indeed, irradiation of cations **2** and **4** with an excess of benzene regenerates crown ethers **1** (96%) and **3** (98%), as well as the starting complex [Cb*Co(C$_6$H$_6$)]$^+$ (ca. 80%).

X-ray Diffraction Study. The structures of complexes **4** and **5** were investigated by X-ray diffraction (Figures 1 and 2). The crown ether moiety in both cases displays a boat conformation with almost orthogonal benzene rings (94.7° for **4**, 91.2° for **5**), which is commonly observed for dibenzo-18-crown-6 species.[10] It should be noted that one of the methyl group carbon atoms is located very close to the center of the crown ether cavity (X) (C···X = 2.143 Å for **4**, 2.641 Å for **5**). This distance is even shorter than that between the cavity center and oxygen atoms (O···X av 2.783 Å for **4**, 2.704 Å for **5**), suggesting that methyl groups might have a steric influence on the binding capacity of **4** and **5**.

The Cb* and benzene rings in **4** are almost parallel to each other (2.8°), with Co···C$_4$ and Co···C$_6$ plane distances being equal to 1.688 and 1.599 Å, respectively. Noteworthy, the

Co···C$_4$ distance in **4** is somewhat shorter and Co···C$_6$ is longer than those in the parent cation [Cb*Co(C$_6$H$_6$)]$^+$ (1.702 and 1.561 Å, respectively)[11] in accordance with the donor effect of the alkoxy substituents. It is also interesting to note that the perimeter of the coordinated benzene ring in **4** (8.426 Å) is significantly larger than that of the noncoordinated one (8.256 Å), due to the interaction with the metal atom.

In contrast to **4**, the cobalt atoms in **5** are nonsymmetrically coordinated to the benzene rings, being notably shifted from the oxygen-substituted carbon atoms (compare for example Co1−C1 2.158 Å and Co1−C3 2.093 Å). This shift can be attributed to the weak electrostatic repulsion of the positively charged cobalt atoms separated by 8.671 Å.

Electrochemistry. In contrast with the well-defined electrochemical activity of the Cb*Co cyclopentadienyl complexes Cb*Co(C$_5$R$_5$),[5a] the present arene derivatives [Cb*Co(arene)]$^+$

(8) For review see: Kudinov, A. R.; Mutseneck, E. V.; Loginov, D. A. *Coord. Chem. Rev.* **2004**, *248*, 571.

(9) All cations were isolated as salts with the PF$_6^-$ anion. The anions are not given in the schemes.

(10) Dapporto, P.; Paoli, P.; Matijašić; Tušek-Božic, L. *Inorg. Chim. Acta* **1996**, *252*, 383.

(11) Mutseneck, E. V.; Loginov, D. A.; Perekalin, D. S.; Pronin, A. A.; Starikova, Z. A.; Petrovskii, P. V.; Kudinov, A. R. *Eur. J. Inorg. Chem.* **2008**, . in preparation.
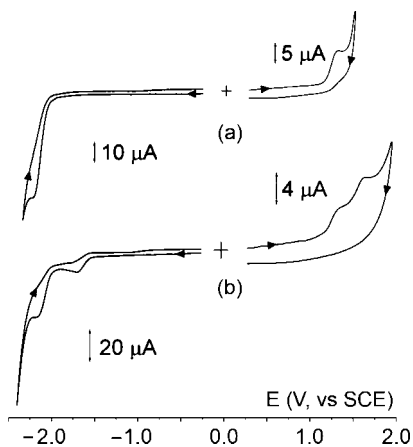
Figure 3. Cyclic voltammetric responses recorded at a glassy carbon electrode in CH$_2$Cl$_2$ solution of (a) **4**PF$_6$ (0.5 × 10^{-3} mol dm^{-3}) and (b) **5**(PF$_6$)$_2$ (0.5 × 10^{-3} mol dm^{-3}). [NBu$_4$][PF$_6$] (0.2 mol dm^{-3}) is the supporting electrolyte. Scan rate is 0.02 V s^{-1}.

Table 1. Peak Potential Values for the Anodic and Cathodic Processes Exhibited by Complexes 2, 4, and 5 in CH$_2$Cl$_2$ Solution

complex	first oxidation $E_{pa}{}^a$	second oxidation $E_{pa}{}^a$	first reduction $E_{pc}{}^a$	second reduction $E_{pc}{}^a$
2	+1.48		−2.18	
4	+1.29		−2.19	
5	+1.36	+1.66	−1.70	−2.17

^{a} From differential pulse voltammetry at 0.02 V s^{-1}.

possess marked incapacity for reversible redox changes. In fact, their redox processes are irreversible and localized at the extreme limits of the anodic and cathodic windows of the employed solvent (CH$_2$Cl$_2$). In addition, their oxidation processes are complicated by electrode adsorption phenomena at different electrodes (platinum, gold, glassy carbon), making necessary the mechanical cleaning of the electrode surface after each voltammetric cycle and giving from time to time not perfectly reproducible results.

As a typical example, Figure 3 shows the cyclic voltammetric behavior of complexes **4** and **5**, recorded at low scan rate and at a freshly polished electrode in order to limit the electrode adsorption phenomena. Complex **4** exhibits either an irreversible oxidation or an irreversible reduction, both processes being close to the solvent discharges. Such a situation prevented obviously the determination of the number of electrons involved in the respective processes by coulometric measurements.

Tentatively, we assign the oxidation to the Co(I)/Co(II) process, in that comparison with an equimolar amount of the one-electron oxidation of [2-di(3,5-xylyl)phosphino]phenyl]-ferrocenyl}ethyldi(3,5-xylyl)phosphine (MW = 770.7) affords a peak height of comparable intensity (see Figure S1 in the Supporting Information). In addition, we intuitively assign the reduction as the Co(I)/Co(0) step.

It is noteworthy that the binuclear complex **5**, even under the mentioned technical difficulties of investigation of the redox processes at increasing scan rates, affords either two separate oxidations or two separate reductions, thus suggesting that the two cobalt centers are electronically interactive.[12] The electrode potentials of the redox processes of complexes **2**, **4**, and **5** are compiled in Table 1.

As a last consideration, we point out that the cyclic voltammetric profiles of the complexes do not show any appreciable
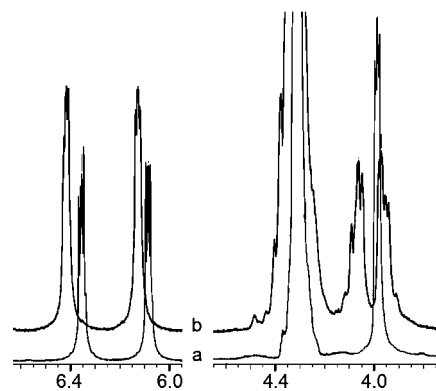
Figure 4. Signals of aromatic (right) and methylene (left) protons of **5**: (a) initial spectrum; (b) spectrum in the presence of a 5-fold excess of Na$^+$. One of the methylene signals overlaps with CD$_3$NO$_2$ residual protons (4.25−4.35 ppm), which is indicated by its broadening in spectrum b.
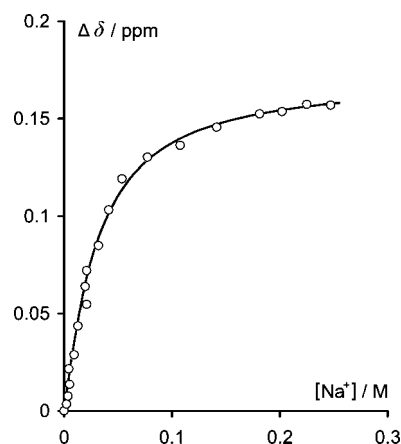
Figure 5. Experimental dots for the changes of aromatic signals ($\Delta\delta$) of **5** and the calculated curve for $K_a = 50$ (pK_a = 1.7). The concentration of **5** is 0.0207 M.

variation in the presence of an excess of NaPF$_6$ salt even in the case of reduction processes, which should decrease the electrostatic repulsion. These results suggest weak coordination of Na$^+$ ions with crown ether derivatives **2**, **4**, and **5**.[13]

Sodium Cation Binding Studies. The association constants (K_a) of the crown ethers **1** and **3** and their cobalt complexes **2**, **4**, and **5** were determined by ^{1}H NMR titration with Na[B(3,5-(CF$_3$)$_2$C$_6$H$_3$)$_4$] in CD$_3$NO$_2$. The typical spectral changes are shown in Figure 4 for complex **5**, as a representative example. The signals of the CH$_2$ groups display the largest shifts (ca. 0.4 ppm) upon sodium complexation; however the complicated splitting makes them useless for K_a measurement. Therefore the signals of aromatic protons were used for this purpose. The changes of these signals ($\Delta\delta$) were plotted against the Na$^+$ concentration, and the resulting experimental dots were fitted with the calculated K_a curve (Figure 5). The K_a of the parent crown ethers **1** and **3** were found to be higher than the upper limit of the NMR titration method ($K_a > 1 \times 10^5$),[14] which correlates with the values 2 × 10^5 and 5 × 10^6 determined by

(12) Zanello, P. *Inorganic Electrochemistry. Theory, Practice and Application*; RSC: UK, 2003.

(13) One of the reviewers noted that the lack of redox shift can also indicate complexation has no effect on the redox properties of the system. See for example: Tucker, J. H. R.; Collinson, S. R. *Chem. Soc. Rev* **2002**, *31*, 147.

(14) For a review on NMR titration methods see: Fielding, L. *Tetrahedron* **2000**, *56*, 6151.

Table 2. Energy Decomposition Analysis of Crown Ether Complexes at BP86/TZ2P (E in kcal mol^{-1})^a.

	fragments	
	Na$^+$ + **3**	Na$^+$ + **4**
ΔE_{Pauli}	12.6	16.0
ΔE_{elstat}	−43.0 (57%)	0.2 (0%)
ΔE_{orb}	−32.5 (43%)	−33.8 (100%)
ΔE_{int}	−75.5	−17.6

^{a} The values in parentheses give the percentage contribution to the total attractive interactions.

conductometry. [15] Much smaller values were found for the cobalt complexes **2** (2500 ± 500), **4** (800 ± 200), and **5** (50 ± 20). These results indicate that π-coordination of the [Cb*Co]$^+$ fragment decreases the sodium-binding capability of the benzocrown ethers by 2−5 orders of magnitude as a result of electrostatic interactions (*vide infra*).

DFT Calculations. In order to get more information about the interaction of [Cb*Co]$^+$ and Na$^+$ cations with dibenzo-18-crown-6 (**3**), we have carried out DFT calculations. At the BP86/TZ2P level (including COSMO solvent corrections for CH$_2$Cl$_2$), the formation of cation **4** from [Cb*Co(C$_6$H$_6$)]$^+$ and crown ether **3** was found to be slightly favorable (2.78 kcal mol^{-1}). This correlates with reversibility of photochemical arene exchange. Interestingly, the formation of dinuclear complex *trans*-**5** appears to be 1.79 kcal mol^{-1} unfavorable. In addition, *trans*-**5** is 2.34 kcal mol^{-1} less stable than the *cis*-isomer, presumably because of the shorter distance between the positively charged cobalt atoms (11.01 and 9.78 Å for *cis*- and *trans*-isomers, respectively). Nevertheless, experimentally, *trans*-**5** is the major product of reaction between [Cb*Co(C$_6$H$_6$)]$^+$ and **3**, suggesting its kinetic origin. Indeed, the conformation of the crown ether moiety in mononuclear complex **4** (see Figure 1) complicates *cis*-attack of the second [Cb*Co]$^+$ fragment, leading to the favorable formation of the *trans*-isomer. Furthermore, *trans*-**5** precipitates from solution, shifting the equilibrium.

The quantitative assessment of association constants for crown ethers still presents a challenge for computational methods, because of the exponential dependence of K_a on energy and the large influence of solvent effects. [16] In order to estimate association constants for **3** and **4** in nitromethane, we have calculated the energy of their reactions with solvated sodium cation [Na(CH$_3$NO$_2$)$_6$]$^+$, additionally using the COSMO model for treatment of general solvent effects. The process proved to be 4.71 kcal mol^{-1} favorable for **3**, which corresponds to K_a = 2700. In sharp contrast, the binding of sodium to **4** requires 8.15 kcal mol^{-1} of additional energy, giving K_a = 1.15 × 10^{-6}. Thus the calculation of K_a values for **3** and **4** gives qualitative rather than quantitative correlation with experiment.

According to the energy decomposition analysis, [17] the interaction of Na$^+$ with cobalt complex **4** (under vacuum) is 57.81 kcal mol^{-1} weaker than with free crown ether **3** (Table 2). This energy difference is solely achieved by dramatic decrease of the electrostatic component, as a result of Coulomb

Table 3. Crystal Data and Structure Refinement Parameters for 4PF$_6$ and 5(PF$_6$)$_2$·(CH$_3$)$_2$CO

	4PF$_6$	**5**(PF$_6$)$_2$·(CH$_3$)$_2$CO
empirical formula	C$_{28}$H$_{36}$CoF$_6$O$_6$P	C$_{39}$H$_{54}$Co$_2$F$_{12}$O$_7$P$_2$
fw	672.47	1042.62
cryst color, habit	yellow plate	yellow prism
cryst size (mm)	0.40 × 0.10 × 0.01	0.38 × 0.35 × 0.29
temp (K)	120(2)	120(2)
cryst syst	triclinic	triclinic
space group	P1$^-$	P1$^-$
a (Å)	9.7460(18)	12.584(6)
b (Å)	12.138(2)	14.088(7)
c (Å)	14.577(3)	15.533(7)
α (deg)	114.113(4)	114.865(16)
β (deg)	106.166(5)	93.39(2)
γ (deg)	91.635(5)	114.21(2)
V (Å^3)	1491.7(5)	2187.7(18)
$Z(Z')$	2(1)	2(1)
$F(000)$	696	1072
D_{calc} (g cm^{-1})	1.497	1.583
linear absorp, μ (cm^{-1})	7.06	9.30
T_{min}/T_{max}	0.7653/0.9930	0.707/0.835
scan type	ω	ω
θ range (deg)	3.57−28.00	1.29−30.00
no. of reflns measd	11 757	14 579
no. of indep reflns	7164 [R_{int} = 0.0867]	10 107 [R_{int} = 0.0482]
obsd reflns [$I > 2\sigma(I)$]	2270	4338
no. of params	383	569
final $R(F_{hkl})$: R_1	0.0663	0.0466
wR_2	0.1985	0.1256
GOF	0.822	0.728
$\Delta\rho_{max}$, $\Delta\rho_{min}$ (e Å^{-3})	0.821, −0.646	0.542, −0.474

repulsion between two cationic centers Co$^+$ and Na$^+$. Interestingly, it appears that sodium is bonded to **4** only by orbital interactions.

Conclusion

Overall, we have demonstrated that photochemically reversible π-complexation of benzocrown ethers by the cationic fragment [Cb*Co]$^+$ decreases their Na$^+$-binding capability by 2−5 orders of magnitude, making them potential molecular switches. The results of DFT calculations show qualitative correlation with K_a values measured by NMR titration and assign the decrease of Na$^+$ binding to the electrostatic repulsion between sodium and cobalt cationic centers.

Experimental Section

General Remarks. All reactions were carried out under argon in anhydrous solvents, which were purified and dried using standard procedures. The isolation of products was conducted in air. The starting cobalt complex [Cb*Co(C$_6$H$_6$)]PF$_6$ was prepared as described in the literature. [5a] Visible light irradiation was performed by a high-pressure mercury vapor lamp with a phosphor-coated bulb (400 W). The ^{1}H NMR spectra were recorded with a Bruker AMX-400 spectrometer at room temperature. Chemical shifts are given in ppm relative to internal SiMe$_4$. Materials and apparatus for electrochemistry have been described elsewhere. [5a] All potential values are referred to the saturated calomel electrode (SCE). Under the present experimental conditions, the one-electron oxidation of ferrocene occurs at $E^{\circ'}$ = +0.39 V. The redox standard [2-di(3,5-xylyl)phosphino]phenyl]ferrocenyl}ethyldi(3,5-xylyl)phosphine was purchased from Aldrich, the ferrocene/ferrocenium oxidation of which is irreversible (E_p = +0.37 V, at 0.05 V s^{-1}).

[Cb*Co(η^6-benzo-15-crown-5)]PF$_6$ ([2]PF$_6$). A mixture of [Cb*Co(C$_6$H$_6$)]PF$_6$ (78 mg, 0.2 mmol) and benzo-15-crown-5 (214 mg, 0.8 mmol) was dissolved in 15 mL of CH$_2$Cl$_2$ and irradiated for 16 h. The solution was then filtered and evaporated under

(15) Inerowicz, H. D.; Chojnacki, J.; Merz, A.; Futterer, T. *J. Incl. Phenom. Macrocyclic Chem.* **2000**, *38*, 123.

(16) (a) Grootenhuis, P. D. J.; Kollman, P. A. *J. Am. Chem. Soc.* **1989**, *111*, 2152. (b) Glendening, E. D.; Feller, D.; Thompson, M. A. *J. Am. Chem. Soc.* **1994**, *116*, 10657. (c) Bagatur'yants, A. A.; Freidzon, A. Y.; Alfimov, M. V.; Baerends, E. J.; Howard, J. A. K.; Kuz'mina, L. G. *THEOCHEM* **2002**, *588*, 55. (d) Stoyanov, E. S.; Reed, C. A. *J. Phys. Chem. A* **2004**, *108*, 907. (e) Sargent, A. L.; Mosley, B. J.; Sibert, J. W. *J. Phys. Chem. A* **2006**, *110*, 3826.

(17) (a) Ziegler, T.; Rauk, A. *Theor. Chim. Acta* **1977**, *46*, 1. (b) Morokuma, K. *J. Chem. Phys.* **1971**, *55*, 1236. (c) Frenking, G.; Fröhlich, N. *Chem. Rev.* **2000**, *100*, 717.

vacuum. The residue was dissolved in acetone and eluted through a short layer of Al_2O_3 (5 cm). Finally crystallization from CH_2Cl_2/Et_2O gives [**2**]PF_6 (60 mg, 51%) as a light yellow powder. ^{1}H NMR: δ 1.65 (s, 12H, C_4Me_4), 3.24 (m, 8H, CH_2), 3.92−3.97 (m, 4H, CH_2), 4.28−4.37 (m, 4H, CH_2), 6.28 (m, 2H, $CoC_6H_4O_2$), 6.64 (m, 2H, $CoC_6H_4O_2$). Anal. Calcd for $C_{22}H_{32}CoF_6O_6P$: C, 44.31; H, 5.41. Found: C, 44.20; H, 5.56.

[Cb*Co(η^6-dibenzo-18-crown-6)]PF_6 ([4]PF_6). A mixture of [Cb*Co(C_6H_6)]PF_6 (78 mg, 0.2 mmol) and benzo-18-crown-6 (288 mg, 0.8 mmol) was dissolved in 20 mL of CH_2Cl_2 and irradiated for 16 h. The solution was then filtered and evaporated under vacuum. The residue was dissolved in acetone and eluted through a short layer of Al_2O_3 (5 cm). Finally crystallization from CH_2Cl_2/Et_2O gives [**4**]PF_6 (95 mg, 71%) as a light yellow powder. ^{1}H NMR ((CD_3)$_2CO$): δ 1.58 (s, 12H, C_4Me_4), 4.00−4.05 (m, 4H, CH_2), 4.13 (m, 4H, CH_2), 4.25 (m, 4H, CH_2), 4.38 (m, 4H, CH_2), 6.24 (m, 2H, $CoC_6H_4O_2$), 6.59 (m, 2H, $CoC_6H_4O_2$), 6.86 (m, 2H, $C_6H_4O_2$), 7.02 (m, 2H, $C_6H_4O_2$). Anal. Calcd for $C_{28}H_{36}CoF_6O_6P$: C, 50.01; H, 5.40. Found: C, 49.87; H, 5.51.

[(Cb*Co)$_2$(η^6,η^6-dibenzo-18-crown-6)](PF_6)$_2$ ([5](PF_6)$_2$). A mixture of [Cb*Co(C_6H_6)]PF_6 (98 mg, 0.25 mmol) and benzo-18-crown-6 (36 mg, 0.1 mmol) was dissolved in 10 mL of CH_2Cl_2 and irradiated for 16 h. The solution was then evaporated to 4 mL and filtered to obtain a yellow-green precipitate. It was dissolved in an acetone/nitromethane (4:1) mixture and eluted through a short layer of Al_2O_3 (5 cm). Slow crystallization from acetone/Et_2O gives [**5**](PF_6)$_2$ (54 mg, 55%) as a bright yellow powder. ^{1}H NMR (CD_3NO_2): δ 1.54 (s, 24H, C_4Me_4), 3.99 (m, 8H, CH_2), 4.32 (m, 8H, CH_2), 6.10 (m, 4H, $C_6H_4O_2$), 6.37 (m, 4H, $C_6H_4O_2$). Anal. Calcd for $C_{36}H_{48}Co_2F_{12}O_6P_2$: C, 43.92; H, 4.91. Found: C, 43.98; H, 4.93.

Reaction of [2]PF_6 and [4]PF_6 with Benzene. Complex [**2**]PF_6 (33 mg, 0.05 mmol) or [**4**]PF_6 (50 mg, 0.05 mmol) was dissolved in 10 mL of CH_2Cl_2 with 0.5 mL of benzene and irradiated for 16 h. The reaction mixture was filtered and the solution was evaporated *in vacuo*. The residue, containing [Cb*Co(C_6H_6)]PF_6 and the corresponding crown ether, was analyzed by ^{1}H NMR spectroscopy.

X-ray Crystallography. X-ray diffraction experiments were carried out with a Bruker SMART 1000 CCD area detector, using graphite-monochromated Mo Kα radiation (λ = 0.71073 Å, ω-scans with a 0.3° step in ω and 10 s per frame exposure) at 120(2) K. The low temperature of the crystals was maintained with a Cryostream (Oxford Cryosystems) open-flow N_2 gas cryostat. Reflection intensities were integrated using SAINT software,[18] and absorption correction was applied semiempirically using the SAD-ABS program.[19] The structures were solved by direct methods and refined by full-matrix least-squares against F^2 in anisotropic approximation for non-hydrogen atoms. The positions of hydrogen atoms were calculated geometrically and refined in isotropic approximation. Crystal data and structure refinement parameters for **4**PF_6 and **5**(PF_6)$_2 \cdot$(CH_3)$_2CO$ are given in Table 3. All calculations were performed using the SHELXTL software.[20]

General Procedure for NMR Titration. To the solution of the crown ether of certain concentration (usually ca. 0.02 M) in CD_3NO_2 was added the sodium salt Na[B(3,5-(CF_3)$_2C_6H_3$)$_4$] in small portions. An ^{1}H NMR spectrum was recorded after each addition. The exact sodium concentration was determined by the integration of the [B(3,5-(CF_3)$_2C_6H_3$)$_4$]$^-$ signals. One initial (no sodium), eight intermediate, and one "saturated" (excess of sodium) spectra were recorded for each sample. The changes of the aromatic signals of the crown ethers were plotted against the Na$^+$ concentration, and the resulting experimental dots were fitted with the calculated K_a curve using MS Excel 2003 software. The chemical shift was represented as $\delta = (C_{\text{free crown}}\delta_{\text{free crown}} + C_{\text{sodium crown complex}}\delta_{\text{sodium crown complex}})/2$, where $\delta_{\text{free crown}}$ was taken from the first experiment (no sodium) and $\delta_{\text{sodium crown complex}}$ from the last one (excess of sodium). Due to low K_a, in the case of **5** $\delta_{\text{sodium crown complex}}$ was assumed to be 0.01 ppm higher than the observed shift at 12-fold excess of sodium.

DFT Calculations. All geometry optimizations were carried out using PRIRODA 6 software.[21] The generalized gradient approximation (GGA) for the exchange−correlation functional by Perdew, Burke, and Ernzerhof (PBE) was employed. The TZVP-quality basis sets of contracted Gaussian-type functions (4s)/[2s] for H, (8s4p1d)/[4s2p1d] for C, O, and N, (14s10p)/[9s5p] for Na, and (17s13p8d)/[12s9p4d] for Co were used. Full optimization of geometries was performed in C_1 symmetry followed by frequency calculation in order to confirm the nature of the stationary points. The resulting geometries (except that of [Na(CH_3NO_2)$_6$]$^+$) were symmetrized to the C_s point group (maximum displacement from this symmetry was 0.003 Å). The final energy was obtained by single-point calculations at the BP86/TZVP2 level in C_s symmetry with ADF2006.01 software[22] including solvent corrections by the COSMO model. The energy decomposition analysis was also performed by ADF2006.01 software. According to this method, the interaction energy $\Delta E_{\text{int}} = \Delta E_{\text{elstat}} + \Delta E_{\text{Pauli}} + \Delta E_{\text{orb}}$, where ΔE_{elstat} is the electrostatic interaction energy between the fragments with a frozen electron density distribution, ΔE_{Pauli} is the repulsive four-electron interactions between occupied orbitals, and ΔE_{orb} is the stabilizing orbital interactions. The visualization of calculation results was performed by ChemCraft software (www.chemcraft-prog.com).

Supporting Information Available: Figure of CVA response of a CH_2Cl_2 solution containing **4** and [2-di(3,5-xylyl)phos-phino]phenyl}ferrocenyl}ethyldi(3,5-xylyl)phosphine. NMR titration curves for **1**−**5**. Details of DFT calculations including Cartesian coordinates and energies. CIF files for the crystal structures of **4**PF_6 and **5**(PF_6)$_2 \cdot$(CH_3)$_2CO$. This material is available free of charge via the Internet at http://pubs.acs.org.

(18) *SMART V5.051 and SAINT V5.00, Area detector control and integration software*; Bruker AXS Inc.: Madison, WI, 1998.
(19) Sheldrick, G. M. *SADABS*; Bruker AXS Inc.: Madison, WI, 1997.
(20) Sheldrick, G. M. *SHELXTL-97*, Version 5.10; Bruker AXS Inc.: Madison, WI, 1997.

(21) (a) Laikov, D. N *Chem. Phys. Lett.* **1997**, *281*, 151. (b) Laikov, D. N. *Chem. Phys. Lett.* **2005**, *416*, 116. (c) Laikov, D. N.; Ustyk, Yu. A. *Russ. Chem. Bull.* **2005**, *54*, 820.
(22) (a) te Velde, G.; Bickelhaupt, F. M.; van Gisbergen, S. J. A.; Fonseca Guerra, C.; Baerends, E. J.; Snijders, J. G.; Ziegler, T. *J. Comput. Chem.* **2001**, *22*, 931. (b) *ADF 2006.01*; SCM, Theoretical Chemistry, Vrije Universiteit: Amsterdam, The Netherlands, http://www.scm.com.